Morphological Evolution of HDPE Parts in the Microinjection Molding: Comparison with Conventional Injection Molding

Chao Guo, Fang Hui Liu, Xian Wu, Hong Liu, Jie Zhang

State Key Laboratory of Polymer Materials Engineering, College of Polymer Science and Engineering, Sichuan University, Chengdu 610065, People's Republic of China

Received 25 May 2011; accepted 24 December 2011
DOI 10.1002/app.36698
Published online in Wiley Online Library (wileyonlinelibrary.com).

ABSTRACT: To compare the difference of morphological evolution of HDPE micropart and macropart, micropart with 200 μm thickness and macropart with 2000 μm thickness were prepared. The PLM images of micropart and macropart exhibited a similar "skin–core" structure, but the micropart showed a much larger fraction of orientation layer. The SEM observation of core layer of micropart featured an unoriented lamellae structure and shear layer of micropart showed a highly oriented shish-kebab structure. The 2D-WAXD patterns of shear layer of macropart indicated twisted oriented shish-kebab (KM-I) structures, however that of micropart indicated untwisted oriented shish-kebab (KM-II) structures which was firstly found in microinjection molding. The diffraction pattern of the micropart exhibited stronger azimuthal dependence than the shear layer of macropart, indicating the most pronounced orientation of HDPE chains within lamellae. © 2012 Wiley Periodicals, Inc. J Appl Polym Sci 000: 000–000, 2012

Key words: morphology; microinjection molding; HDPE; conventional injection

INTRODUCTION

The miniaturization of parts is a necessary step for technological progress, where more functions must be integrated into a smaller space. With the rapid development of microengineering technologies, there is an increasing trend towards product miniaturization, and now the use of plastic microstructured parts in the field of microelectromechanical systems (MEMS) has been greatly increasing over the past decades because of their versatility and ease of batch fabrication.[1–3] Microinjection molding (MIM) is one of the most suitable processes for replicating microstructured parts cheaply and with high precision among a variety of polymer processing methods. Many micro and microfeatured products, such as micro sampling cells, micro heat exchangers, micro pumps, biochips, and optical grating elements have been successfully injection molded.[4,5] Parts manufactured by microinjection molding fall in one of the following three categories: Type A is parts with microweights in the milligram range; Type B is parts with microstructured regions which are characterized by local microfeatures on the order of microns, such as microholes and slots; Type C is parts exhibiting dimensional tolerances in the micrometer range but without dimension limit.[6–8]

The microinjection molding is not simply a scaling down of the conventional injection molding, but needs some important changes in methods and practices. Specific conditions should be chosen for a good replication of microparts.[7] Lots of studies have investigated the effects of the main process parameters on the micro molding process, including mold temperature, injection speed and pressure, holding time, and holding pressure.[8–11] However, the current knowledge regarding the influence of microinjection molding on polymers is not yet clearly defined, and only a few researches on the morphology and properties of the polymer microparts molded by microinjection are available.[7] The morphologies of semicrystalline materials strongly affect their physical properties (mechanical, optical, electrical, transport, and chemical), and accordingly the control of the structural hierarchy from subnanometer- to micrometer-length scales is thus important technologically and fascinating scientifically.[12,13]

High density polyethylene (HDPE), as a semicrystalline polymer, represents one of the most commonly used polymeric materials. Flow-induced crystallization of HDPE can lead to the formation of

Correspondence to: J. Zhang (zhangjie@scu.edu.cn).
Contract grant sponsor: National Natural Science Foundation of China; contract grant numbers: 50873072, 51010004.
Contract grant sponsor: Sichuan Science and Technology Support Project.

special structures, called shish-kebab lamellae row structures,[14] which have been found in injection molding, gas-assisted injection molding, blow molding, and drawing processes.[15–18] The formation of these structures involves the following steps: shear flow implies an alignment of polymer chains in the shear direction, which will form fibril-like structures called "shish" as soon as the crystallization temperature is reached. The folded chain lamellae will grow epitaxially on these "shishes," which finally form "kebabs." The lamellar orientation of kebabs depends on the nature of flow. For HDPE, skin and shear layers generally exhibit "shish-kebab" structure, with kebab lamellae twisted along the growth direction due to chain tilting.[19] This morphology is identified as a "KM-I" morphology according to Keller-Machin,s models.[20,21] As for high molecular weight HDPE and/or high shear stresses, a "KM-II" morphology has been observed by different authors, where the chains composing kebab are aligned in the shear direction.[20,21] But the "KM-II" morphology has never been found in microinjection molding before.[22] These different morphologies can be detected through the help of WAXD or SAXS experiments.

For microparts, the thickness is reduced sometimes to a few hundredths of a micron, which dictates many processing features of microinjection molding different from conventional injection molding, such as higher injection pressure and speed, higher melt and mold temperature, etc. The specific thermomechanical environment dictated by the micro scale size in microinjection molding and resulting rheological behavior of flow can affect the various steps of crystallization of semicrystalline polymers (i.e., nucleation and growth of crystalline lamellae), resulting in a specific morphological feature different from that of macropart prepared via conventional injection molding. In order to probe their morphological differences, a macropart with a thickness of 2 mm and a micropart with a thickness of 200 μm were prepared in this study. Special attention was paid to their morphological comparison by means of optical, thermal, and x-ray diffraction measurements.

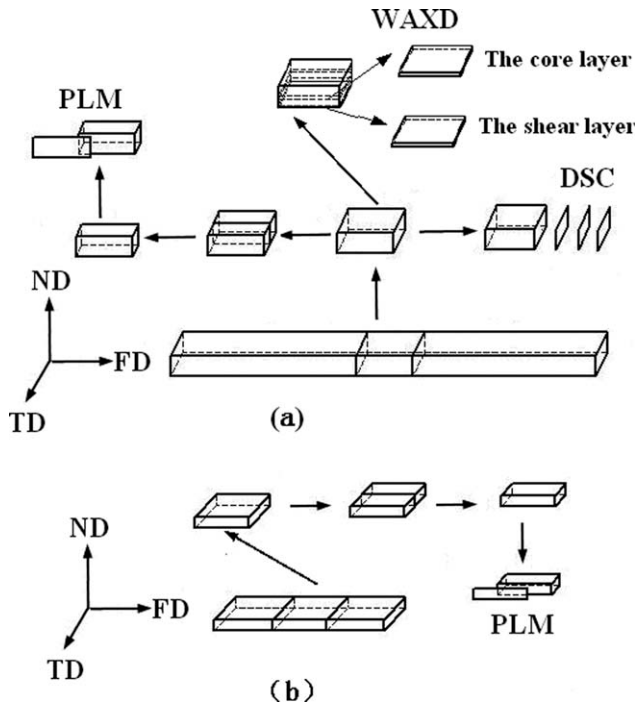

Figure 1 Schematic drawing of sampling methods for each analyses: (a), macropart (2 mm thick); (b), micropart (200 μm thick). Entire part is used in the DSC and WAXD analyses for micropart. FD, flow direction; TD, transverse direction; ND, normal direction.

EXPERIMENTAL

Material

A commercially available HDPE (trade marked as 6098, Qi Lu Petroleum China) was used in this study. Its average molecular weight is (M_w) 6.73 × 10^5 g/mol; its polydispersity index is 4.26 and its melt flow rate (MFW) is 14 g/10 min.

Sample preparation

Two kinds of parts (micropart and macropart) with the similar rectangular geometries but different dimension size were prepared. The micropart, with dimension of 6 × 4 × 0.2 mm^3, was defined as a part with weight (7.15 mg) in the range of few milligrams, and dimensions and tolerances in the micrometer range.[6–8] The dimension of macropart was 80 × 40 × 2 mm^3 and the scheme of macropart and micropart are shown in Figure 1(a,b), respectively.

Both micropart and macropart were injection-molded by a HAAKE MiniJet Piston Injection Molding System, which is very flexible to injection-molded specimens with different geometries and dimension size by customizing desired mold, and provides simplistic handling with consistent, reproducible results. This Injection Molding System is manufactured by Thermo Scientific based on Germany which can provide a whole set of integrated laboratory workflow solutions. In order to eliminate the influence of different process parameters on results, the injection molding parameters of macropart were applied as the same as the micropart. The melt and mold temperatures were respectively 250 and 130°C, the injection time was 1 s, the injection pressure was 100 MPa, the packing pressure was 80 MPa, the hold time was 10 s, and the cooling time was 30 s. When the injection time is 1 s, the mold to shape the macropart will be filled entirely. So the injection rate (Q) is 6.4 cm^3/s. and the flow rate is about 6.1 g/s.

The apparent shear rate in the rectangular cavity can be calculated according to

$$\dot{\gamma} = \frac{6Q}{wh^2} \quad (1)$$

where Q is injection rate; w and h is the width and height of the mould cavity respectively. For the macropart, w and h is 40 and 2 mm, respectively, the apparent shear rate is 240 s^{-1}. For the micropart, the injection rate is the same as the macropart; w and h is 4 and 0.2 mm, respectively, the apparent shear rate is 2.4×10^5 s^{-1}. So the apparent shear rate for the micropart is much larger than that for the macropart.

In this experiment a cone-shaped mold was used. The gates of the mold for the micro and macropart are both square and have the same dimension: $6 \times 4 \times 2$ mm^3. When the injection and packing processes were finished, we moved the mold out from the heating stove and made it cooled at room temperature. It should be noted that in the HAAKE MiniJet Piston Injection Molding System, the parameter of injection time is not the actual injection time. Within the setting injection time a fixed amount of resin will be injected to the mold and when the mold was filled entirely the piston will stopped automatically. For the macropart the actual injection time is the injection time. But for the micropart the actual injection time is much shorter than the injection time. The same injection time indicates the same injection rate.

PLM observation

Polarized light optical microscopy was used to visualize structural layers over the thickness of the sample. Thin slices analyzed by polarized light optical microscopy were cut by means of a microtome. The sampling zones of both micropart and macropart were located in the middle of sample, as shown in Figure 1. Polarized light microscopy observations were performed with a DX-1(Jiang Xi Phoenix Optical, China.) microscope with 45° cross-polarized light, connected with a Nikon 500D digital camera. In order to make a quantitative evaluation of thickness of each layers, the thickness of the different layers, t, their relative thickness, t_r (ratio between the thickness t and the total thickness t_T, which were 2000 and 200 μm for macropart and micropart, respectively) and the relative thickness of the oriented region (t_{ro}) were evaluated.

SEM analysis

To better characterize the morphology which is not very clear in PLM observations, slices were chemically etched in a permanganate etching solution and then observed using scanning electronic microscopy. The solution was a mixture of 8 : 4 : 1 volume of concentrated sulfuric acid, phosphoric acid, and distilled water, respectively (1.5 g of potassium permanganate in 100 mL of mixture). The sampling zones for both two parts were the same as PLM observation. A Hitachi scanning microscopy (Model S-450, Hitachi, Osaka, Japan) was used for the SEM measurements. Prior to microscopy examination, the surfaces of the samples were coated with a thin layer of gold by ion sputtering.

DSC analysis

Differential scanning calorimetry (DSC) experiments were performed by a Perkin–Elmer differential scanning calorimeter (Model Pyris 1, Perkin Elmer Cetus Instruments, Norwalk, CT) using N_2 as purge gas at a heating rate of 20°C/min. About 6–8 mg of the macropart and entire micropart were used for DSC measurements. It should be noted that the whole thickness is sampled for micropart in order to a better comparison with the macropart, and the sampling zone of macropart is shown in Figure 1(a). From heating scans, melting temperature and degree of crystallinity were determined.

The degree of crystallinity (X_i) of HDPE can be calculated according to

$$X_i = \frac{\Delta H_i}{\Delta H_i^{\theta}} \times 100\% \quad (2)$$

where ΔH_i is the calibrated specific fusion heat; ΔH_i^{θ} is the standard fusion heat HDPE, being 170 J/g.

Synchrotron two-dimensional wide-angle X-ray diffraction

The two-dimensional 2D WAXD experiments were carried out at room temperature upon the U7B beam line in the National Synchrotron Radiation Laboratory (NSRL), University of Science and Technology of China, Hefei. The wavelength used is 0.1548 nm and the sample-to-detector distance was 315 mm. The 2D WAXD patterns were recorded in every 180 s by a Mar CCD 165 X-ray detector system. The samples were placed with the orientation (flow direction) perpendicular to the beams. All the 2D WAXD patterns given in this study have been extracted the background thus allows a qualitative comparison between different samples. The Fit2D software package was used to analyze the 2D WAXD patterns. It should be noted that two layers, i.e., the shear layer and core layer, were respectively sampled along flow direction for macropart in WAXD analysis due to the diffraction characteristics

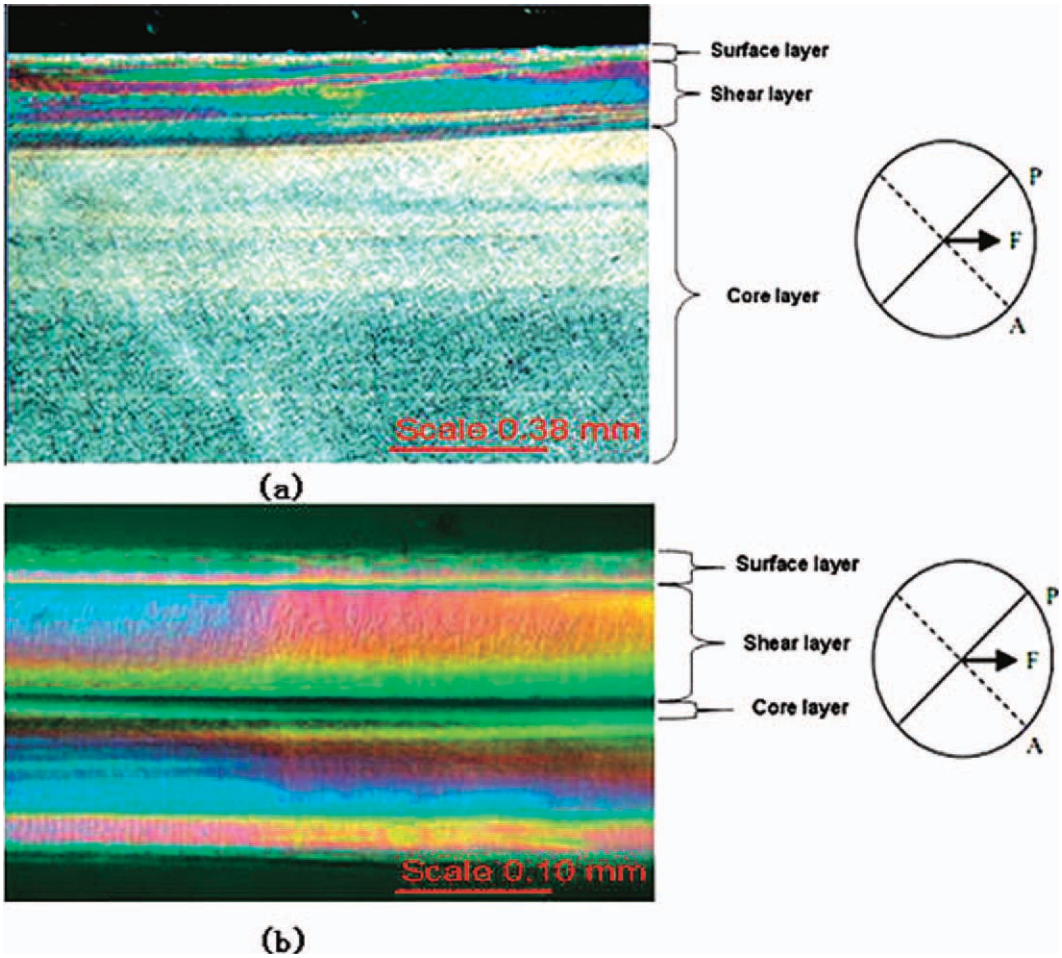

Figure 2 PLM micrographs of macropart and macropart : (a) the half cross-section of the molded macropart (b) the whole cross-section of the micropart (about 200 μm). The flow direction is horizontal. [Color figure can be viewed in the online issue, which is available at wileyonlinelibrary.com.]

of the penetration and its thickness of 2000 μm. The sampling zone and method of the macropart is shown in Figure 1(a). Entire micropart was used in this experiment. From the 2D WAXD patterns. the circularly averaged one-dimensional (1D) WAXD intensity profile was obtained.

The degree of crystallinity, X_c, can be also determined from the WAXD patterns based on the ratio of the integrated intensities under the crystalline peaks A_c to the integrated total intensities, $A = A_c + A_a$ in which A_a is the integrated intensities under the amorphous halo.

$$X_c = \frac{A_c}{A_c + A_a} \times 100\% \quad (3)$$

RESULTS AND DISCUSSION

Microscope

Figure 2 compares optical micrographs of cross-sections of the macropart, Figure 2(a), and the micropart, Figure 2(b). Schematic models for the alignment of the samples between crossed polarizer are shown on the right: "A" represents the analyzer; "P" represents the polarizer; "F" represents the flow direction. A typical morphology distribution of an injection molded semicrystalline sample can be observed in both the parts. In the case of the macropart, three distinctive layers can be observed: a thin, oriented skin layer; a highly oriented zone (often referred as "shear layer"); and a core with essentially no preferred oriented lamellae (often referred as "core layer"). For the micropart, as shown in Figure 2(b), a similar "skin–core" structure was found regardless of the thickness fraction of each layer. To better characterize the skin-core structure, slices of the micropart were chemically etched according to Figure 1 and then observed using scanning electronic microscope. Two SEM micrographs were reported in Figure 3: the first micrograph refers to the shear layer of Figure 2(b), the second one to the central layer. SEM observations confirm the results obtained from optical microscope: in the central

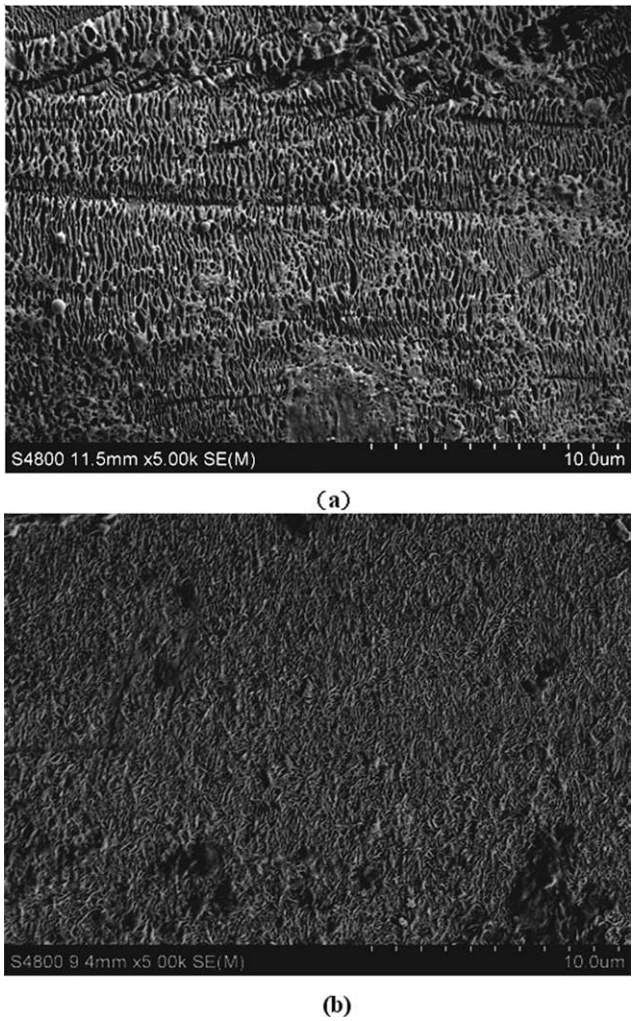

Figure 3 SEM micrographs for the micropart (a) shear layer, 200 μm from the skin (b) core layer, midplane.

layer, an unoriented lamellae crystal structure was observed [Fig. 3(b)] while inside the shear layer of the Figure 2(b) a highly oriented shish-kebab structure was observed [Fig. 3(a)]. This is consistent with literature,[14] which reported the shish-kebab structure in the shear zone of HDPE sample prepared by conventional injection molding.

The thickness of the different layers, t, their relative thickness, t_r and the relative thickness of the oriented region (t_{ro}) were shown in Table I, from which it can be noted that the thicknesses of the "skin" layer and "core" layer were comparable for the two parts, taking into account the experimental uncertainties. However, the relative thicknesses of each layer were quite different. For the macropart, the relative thickness of the shear layer was about 16%, while that of micropart was about 72%. The relative thickness of the oriented layer of micropart, which included both the skin layer and the shear layer, was greatly thicker than that of the macropart (90% VS 20%). It has been proved by many studies that the oriented layers have a great effect on the mechanical strength. The tensile yield strength, impact strength, and tensile modulus increase with increasing the thickness of oriented region: According to the study by Qiang Fu et al.[23] the tensile strength of pure HDPE is greatly enhanced to 125 MPa from 30 MPa because the proportion of oriented layer was enhanced via dynamic packing injection molding. The final mechanical performance of injection-molded parts is mainly dependent on the skin-core ratio, the level of orientation, and the degree of crystallinity.[24,25] Accordingly, the larger oriented region of micropart indicates a good mechanical performance. But the larger oriented region may result in warpage because of the uneven shrinkage in the molding process.

During the filling stage of the injection molding, the molten HDPE is injected into a mold, contacting the mold wall and forming a layer of solidified material instantaneously, known as "skin layer". The formation of the "skin layer" not only reduces the flow cross-section area but also promotes the creation of a thermal insulating barrier for the central molten polymer, leading to an increase in the shear stresses and a decrease in the cooling rates respectively. These effects promote the flow-induced crystallization, and in particular the formation of highly oriented lamellar structures in this region (shear layer). In flow, the polymer chains with high molecular weight were stretched in the direction of the shear field and formed an oriented structure. The oriented structure (microfibrils or shish) parallel to the flow direction is able to orient into fibrous crystals acting as nucleating threads for the lower molecular weight chain, which relax much faster during and after flow. Lamellae over growth takes place on these oriented threads, resulting in a shish-kebab structure. The previously crystallized HDPE, which composed of the solid frozen layer (the skin layer and shear layer), act as a insulation barrier due to its low thermal conductivity, leading to a slower cooling rate in the core and allowing the relaxation of previously oriented chains formed in filling stage or

TABLE I
Comparison of the Absolute and Relative Thicknesses of Different Layers of Macropart and Micropart

	Layer	Thickness t (μm)	Relative thickness t_r (%)	Relative thickness of oriented region t_{ro} (%)
Macropart	Skin	40 ± 10	4(±1)	20(±3)
	Shear	160 ± 20	16(±2)	
	Core	800 ± 30	80(±3)	
Micropart	Skin	35 ± 6	18(±3)	90(±6.5)
	Shear	145 ± 10	72(±5)	
	Core	20 ± 6	10(±3)	

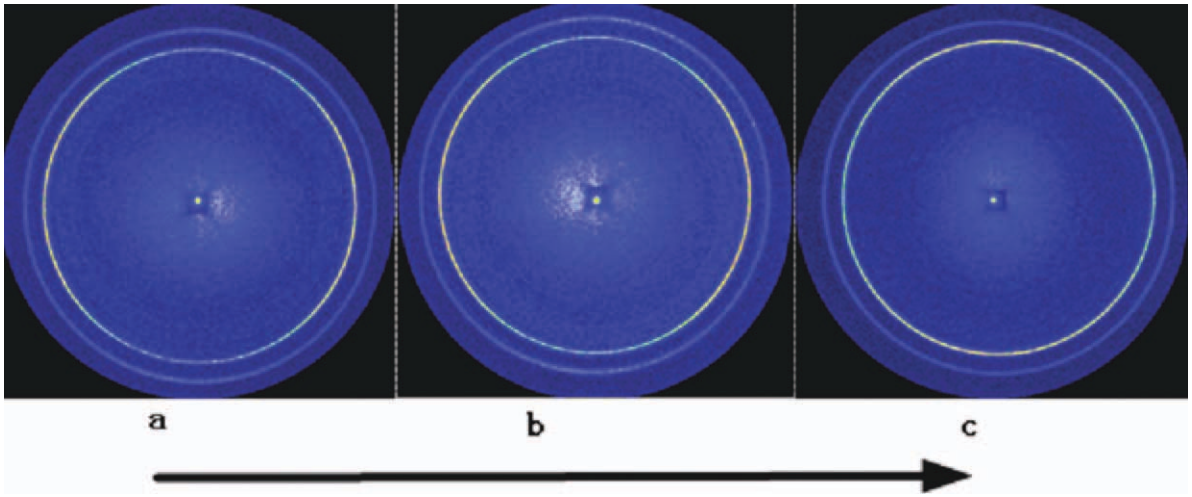

Figure 4 2D-WAXD images corresponding to the three different layers for the macropart: (a) surface layer (b) shear layer (c) core layer. The flow direction is horizontal. [Color figure can be viewed in the online issue, which is available at wileyonlinelibrary.com.]

holding stage. Crystallization then occurs under quiescent-like conditions resulting in an unoriented lamellar morphology in this layer (core layer).

The thermomechanical environment imposed upon the material during injection molding involves thermal gradients, stress levels, and their local variations through the spatial domain of the molding, which can strongly affect the morphological distribution of HDPE parts. For the micropart, the higher shear rates and cooling rates due to microsized cavity favor the formation of oriented structures. Accordingly, the fraction of the oriented structures formed during microinjection molding is higher than that formed during conventional injection molding. The large fraction of oriented structures promotes nucleation resulting in a final morphology of micropart with a large fraction of oriented region or "shish-kebab" structures.

Crystalline morphology and orientation

The 2D-WAXD images corresponding to the three different layers for the macropart and to the whole sample for the micropart were shown in the Figures 4 and 5, respectively. The positions of the diffraction peaks for two samples are similar, in which the following crystallographic planes were analyzed: (110) and (200), corresponding to the diffraction angles $2\theta = 21.5°$, $24.1°$, respectively. From Figure 4(a) which is corresponding to the skin layer and Figure 4(b) which is corresponding to the shear layer for the macropart, we can find that (110) reflections of the crystal lattice planes exhibit azimuthal dependence in the equatorial direction and (200) reflection in the meridian direction. However from Figure 5, which is corresponding to micropart, the (110) and (200) reflections both exhibit azimuthal dependence in the equatorial direction. According to the models proposed by Keller-Machin,[20,21] the diffraction pattern of Figure 4(a,b) and its associated intensity profile can be related to the formation of shish-kebab morphology with twisted lamellae, called the "KM-I" model. A scheme of KM-I morphology is proposed in Figure 6, in accordance with Nagasawa et al. study.[19] KM-I morphology is thus dominant in the orientation layer (surface layer and shear layer) for the macropart. The diffraction pattern of Figure 5 and its associated intensity profile can be related to the formation of shish-kebab morphology with untwisted lamellae, called the "KM-II" model,[20,21] as shown in Figure 7. It was proposed by Keller et al. that "KM-II" model can be developed at high shear rate, as we would expected in the microinjection molding.[19] Mendoza confirmed this assumption by showing the formation of "KM-II"

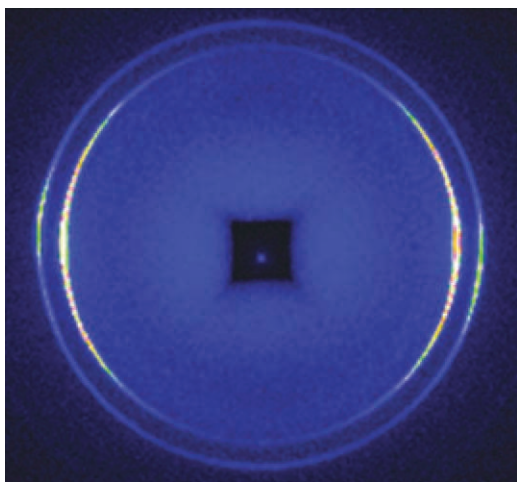

Figure 5 2D-WAXD image for the micropart. [Color figure can be viewed in the online issue, which is available at wileyonlinelibrary.com.]

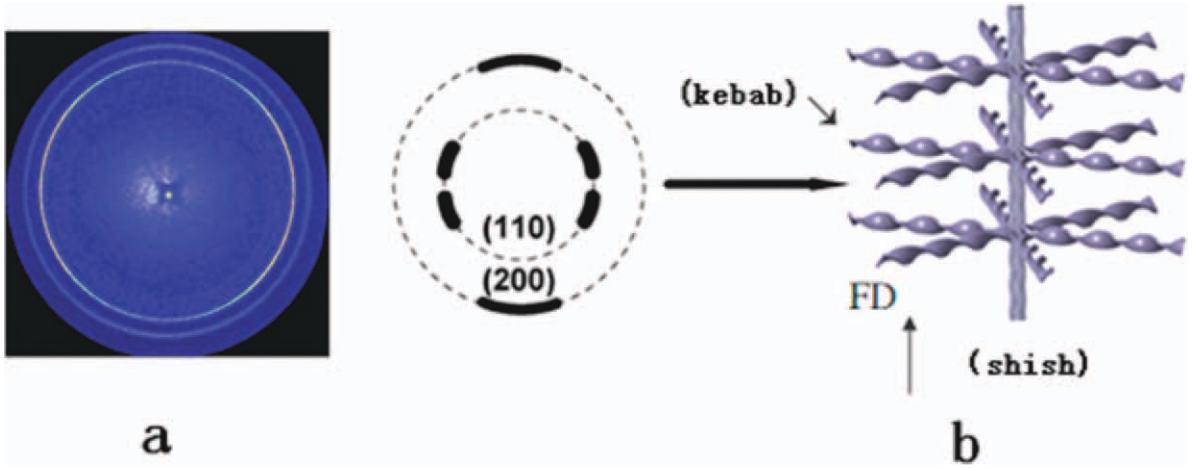

Figure 6 2D-WAXD patterns (a) for the macropart indicating typical oriented WAXD patterns (b) of shish-kebab structures with twisted lamellae (KM-I) according to Keller and Machin. [Color figure can be viewed in the online issue, which is available at wileyonlinelibrary.com.]

morphology for a 1mm thick injection molded plate,[26] but this morphology was firstly found in the microinjection molding in this study. The pattern of Figure 4(c) corresponding to the core layer of macropart shows full Debye rings of (110) and (200) reflection of the crystallattice planes, indicating a completely unoriented lamellae crystal structure.

In the injection molding, the polymer chains with high molecular weight, which has the largest relaxation time, is able to orient into fibrous crystals acting as nucleating threads for the lower molecular weight part, which relax much faster during and after flow. Lamellar overgrowth takes place on these oriented threads, resulting in a shish-kebab structure. The degree of stretch can affect not only the number of nucleating threads (shish) but also the configuration of the transversely growing lamellae (kebabs).[17] For microparts, the thickness is reduced sometimes to a few hundredths of a micron, which dictate many processing features of microinjection molding differing from conventional injection molding, such as higher injection pressure and speed, higher melt, and mold temperature, etc. So the higher shear rate and cooling speed resulted from the specific processing conditions in microinjection molding may promote the formation of this special untwisted oriented morphology, as shown in Figure 7(b).

From 2D-WAXD images we can evaluate the orientation of the crystal planes. For the macropart, the pattern of the core layer presented full Debye rings, which indicates nearly completely unoriented, as shown in Figure 4(c). The pattern of the orientation layer (shear layer and surface layer) exhibited azimuthal dependence, which indicates obvious orientation, as shown in Figure 4(a,b). For the micropart, the rings identified for the micropart from the inner to the outer ring are the same as the macropart but the diffraction pattern exhibited stronger azimuthal dependence.

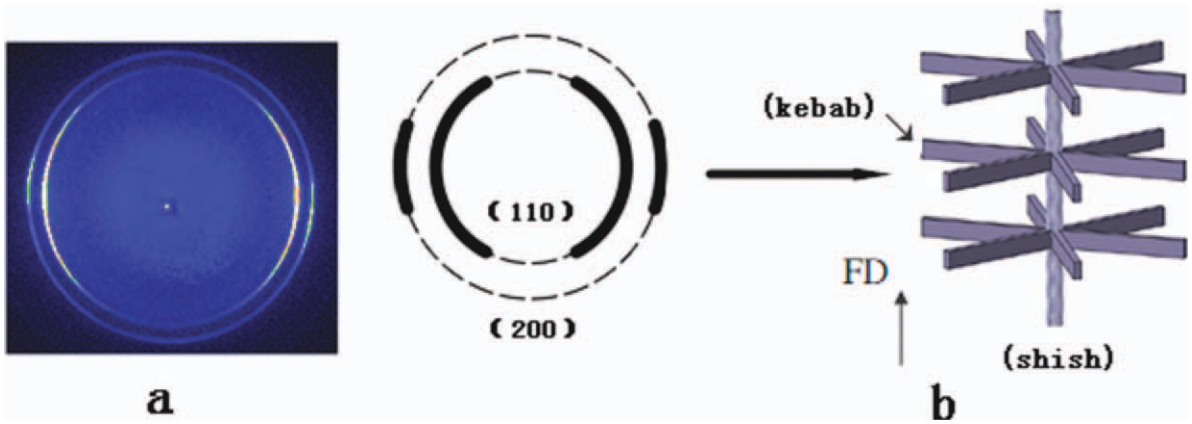

Figure 7 2D-WAXD patterns (a) for the micropart indicating typical oriented WAXD patterns (b) of shish-kebab structures with untwisted lamellae (KM-II) according to Keller and Machin. [Color figure can be viewed in the online issue, which is available at wileyonlinelibrary.com.]

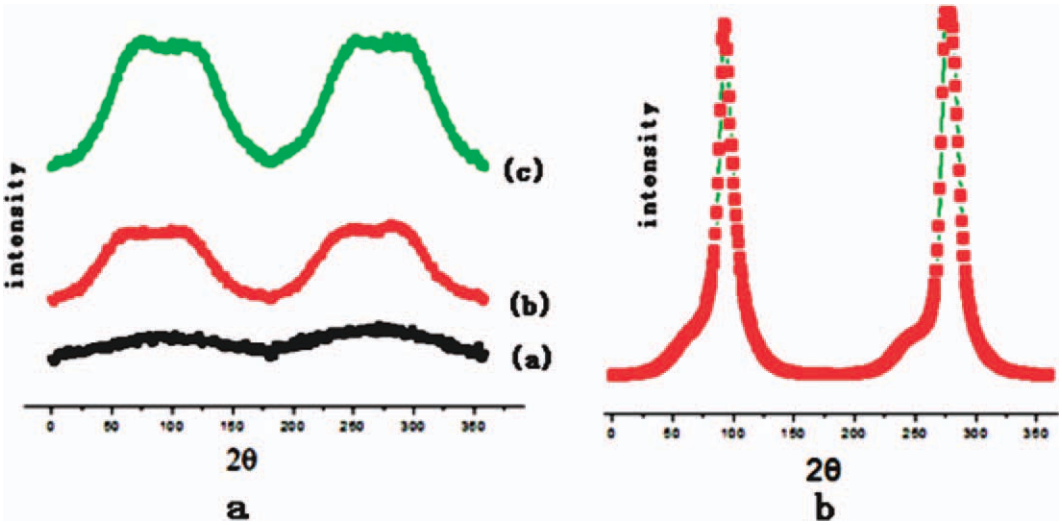

Figure 8 The azimuthal profiles of (110) reflection: a, the macropart: (a) the core layer; (b) the surface layer; (c), the shear layer of macropart. b, The micropart. The flow direction is vertical. [Color figure can be viewed in the online issue, which is available at wileyonlinelibrary.com.]

Using the Hermans orientation function, the orientation level of various planes could be quantitatively evaluated according to

$$f = \frac{3\langle \cos^2 \varphi \rangle - 1}{2} \tag{4}$$

$$\langle \cos^2 \varphi \rangle = \frac{\int_0^{\frac{\pi}{2}} I(\phi) \sin \phi \cos^2 \phi d\phi}{\int_0^{\frac{\pi}{2}} I(\phi) \sin \phi d\phi} \tag{5}$$

where φ is the angel between the normal of a given (*hkl*) crystal plane and shear flow direction, and I is the intensity. Its limiting values of orientation parameter f, taking $\varphi = 0$ as the shear flow direction, are -0.5 for a perfectly perpendicular orientation and 1.0 for a perfectly parallel orientation. An unoriented sample gives $f = 0$.

The (110) reflection in this study is chosen to quantitatively evaluate the orientation level of macropart and micropart. The intensities of the reflection were plotted against the azimuth angle from 0° to 360°, in which 0° represents the equatorial (ND) direction, as shown in Figure 8. The orientation parameters estimated are listed in Table II. In the core layer of macropart, the orientation parameters tend to zero (0.02), which clearly implies the random orientation presented in this layer. It is consistent with the presence of unoriented lamellae crystal structure as shown in Figure 2. While in the orientation layer (shear layer and surface layer) the orientation parameters are much higher, indicating pronounced orientation in these layers. Meanwhile the orientation parameter of the shear layer is a little higher than the surface layer because of the increase in the shear stresses and the decrease in the cooling rate in the shear layer. For the micropart, the highest orientation parameter indicates the most pronounced orientation of HDPE chains within lamellae. The higher shear rates and faster cooling speeds (due to reduced thickness) can explain the highest orientation parameter, both of which are favorable to the formation of highly oriented structures, resulting in more oriented structures than that formed in the macropart.

TABLE II
Orientation Parameter Estimated from Azimuthal WAXD Pattern of (110) Reflection

	Micropart	Surface layer of macropart	Shear layer of macropart	Core layer of macropart
f	0.97	0.42	0.54	0.02

Crystallinity

The DSC curves of macropart and micropart were depicted in Figure 9, which are related to the

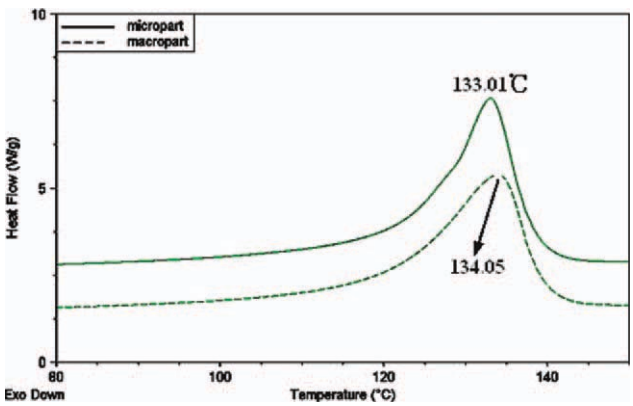

Figure 9 DSC curves for the micropart and macropart. [Color figure can be viewed in the online issue, which is available at wileyonlinelibrary.com.]

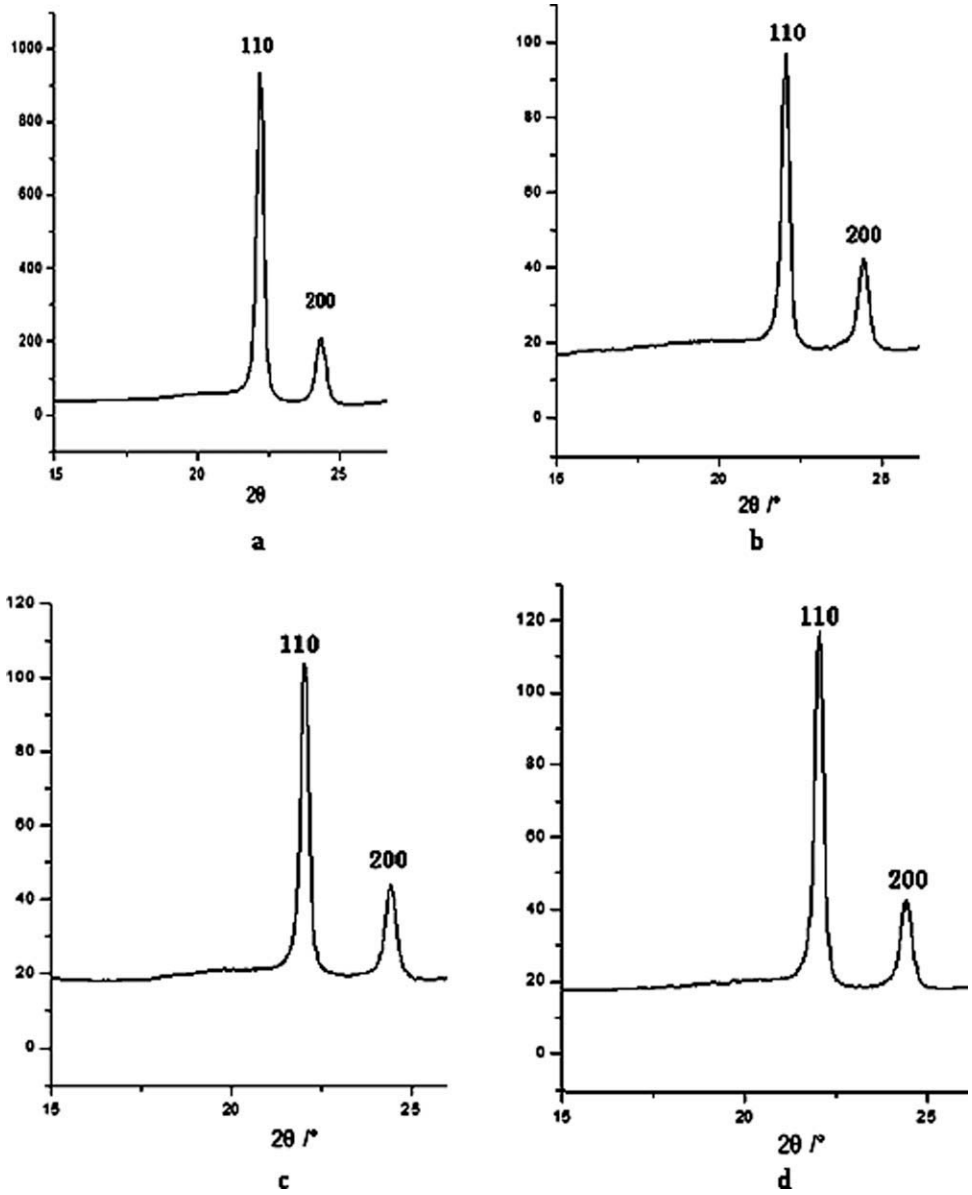

Figure 10 1D WAXD patterns of macropart and micropart: a, micropart; b, the surface layer of macropart, c, the shear layer of macropart d, the core layer of macropart.

melting of the crystalline lamellae. The peak corresponding to the micropart is thinner, indicating a more homogeneous distribution of lamellae thickness. From the 2D WAXD patterns, the circularly averaged one-dimensional (1D) WAXD intensity profiles was obtained as shown in Figure 10. In the WAXD profile of HDPE, the following reflections are usually expected: (110) at $2\theta = 21.5°$, (200) at 24.1°. Table III shows the degree of crystallinity of macropart and micropart obtained from both the DSC and WAXD analysis. It is noted that the values of the crystallinity obtained from the WAXD analysis were a little higher than that from DSC measurement for both macropart and micropart. This difference of the results can originate from the fact that X_c determined by the DSC technique is calculated from the signal recorded during the heating, during which a partial loss of orientation in DSC scanning may occur due to the heating which implies relaxation of chains. Comparatively, 1D WAXD analyses, performed at ambient temperature, give a real

TABLE III
Crystallinity of Macropart and Micropart Obtained from the DSC and WAXD Analysis

		DSC	WAXD
Macropart	Surface layer	55.75%	62.31%
	Shear layer		63.48%
	Core layer		65.33%
Micropart		63.73%	71.33%

illustration of crystalline morphology. Generally speaking, the crystallinity based upon WAXD data is more accurate. But the diffracted pattern is also influenced by the possible orientation of crystal planes, which influences the calculated X_c and may result in the higher values obtained from WAXD. However, they are acceptable to a relative comparison and the change trend of the crystallinity based upon DSC is in accordance with that based on the WAXD data.

From Table III one can observe that the degree of crystallinity of the micropart were higher than that of macropart. For the micropart, the higher degree of crystallinity and the more homogeneous distribution of lamellae thickness are attributed to the increase in the nucleation density in this study. Two origins can be proposed to explain the increase in the nucleation density. One is the higher relative amount of HDPE melt which is in contact with the mold walls for the micropart. The amount of this kind of HDPE melt increases with the ratio of surface area and volume, which promotes the number of nuclei for the micropart, compared with that of the macropart.[27] The other is higher effect of flow-induced crystallization, i.e., the orientation promotes nucleation, resulting in a greater number of smaller crystals.[22,28,29] The high shear rate in microinjection molding favors the alignment of polymer chains along the flow direction, and formed a relatively large fraction of oriented structures. The orientation with large fraction pronouncedly promotes nucleation and subsequently growth of crystalline lamellae.

CONCLUSIONS

The morphologies of HDPE micropart (200 μm thick) and macropart (2000 μm thick) were compared by means of optical, thermal, and X-ray diffraction measurements. The PLM images of micropart and macropart exhibited a similar "skin–core" structure, but the micropart showed a much larger fraction of orientation layer. The SEM observation of shear layer of micropart featured highly oriented shish-kebab structures and the core layer showed an unoriented lamellae crystal structure. The 2D-WAXD patterns of macropart indicated a twisted oriented shish-kebab (KM-I) structure, while that of micropart indicated an untwisted oriented shish-kebab (KM-II) structure which was firstly found in microinjection molding in this study. The degree of crystallinity of micropart was higher than that of the macropart. The 2D WAXD pattern of the core layer of macropart shows full Debye rings, indicating a random orientation. While the orientation layer exhibits strong azimuthal dependence, indicating a pronounced orientation. The diffraction pattern of the micropart exhibits stronger azimuthal dependence than the shear layer of the macropart, with the highest orientation parameter, indicating the most pronounced orientation of HDPE chains within lamellae.

The specific thermomechanical environment in microinjection molding resulted in the specific morphology of the micropart differing from the macropart. The strength of shear stress, can affect not only the number of nucleating threads (shish) but also the configuration of the transversely growing lamellae (kebabs). Because of the reduced thickness of the micropart, the shear rate and cooling speed were higher in microinjection molding than in conventional injection molding, promoting the formation of this special untwisted oriented morphology (KM-I). The specific morphological feature of the microparts indicates specific physical properties differing from that of the macroparts, for example, the large fraction of oriented region of the microparts indicates a good mechanical performance.

The authors are indebted to the National Synchrotron Radiation Laboratory (NSRL) in University of Science and Technology of China and Prof. Guo qiang Pan (NSRL) for his help in synchrotron WAXD experiment.

References

1. Monkkonen, K.; Hietala, J.; Paakkonen, P.; Paakkonen, E. J.; Kaikuranta, T.; Pakkanen, T. T.; Jaaskelainen, T. Polym Eng Sci 2002, 42, 1600.
2. Yu, L.; Lee, L. J.; Koelling, K. W. Polym Eng Sci 2004, 44, 1866.
3. Zhang, K. F.; Lu, Z. Microsyst Technol 2008, 14, 209.
4. Rean, D. C.; Wen, R. J.; Shia, C. C. J Micromech Microeng 2005, 15, 1389.
5. Huang, C. K.; Chiu, S. J Appl Polym Sci 2005, 98, 1865.
6. Despa, M. S.; Kelly, K. W.; Collier, J. R. Microsyst Technol 1999, 6, 60.
7. Giboz, J.; Copponnex, T.; Mélé, P. J Micromech Microeng 2007, 17, 96.
8. Whiteside, B. R.; Martyn, M. T.; Coates, R. D. Int Polym Proc 2005, 20, 162.
9. Zhao, J.; Mayes, R. H.; Chen, G.; Xie, H.; Chan, P. S. Polym Eng Sci 2003, 43 1542.
10. Zhao, J.; Mayes, R. H.; Chen, G.; Chan, P. S.; Xiong, Z. J. Plast Rubber Compos 2003, 32, 240.
11. Chu, J. S.; Kamal, M. R.; Derdouri, S.; Hrymak, A. Polym Eng Sci 2010, 50, 1214.
12. Pantani, R.; Coccorullo, I.; Speranza, V.; Titomanlio, G. Prog Polym Sci 2005, 30, 1185.
13. Kimata, S.; Sakurai, T.; Nozue, Y.; Kasahara, T.; Yamaguchi, N.; Karino, T.; Shibayama, M.; Kornfield, J. A. Science 2007, 316, 1014.
14. Wang, K.; Chen, F.; Zhang, Q.; Fu, Q. Polymer 2008, 49, 4745.
15. Schrauwen, B. A. G.; Von Breemen, L. C. A.; Spoelstra, A. B.; Govaert, L. E.; Peters, G. W. M.; Meijer, H. E. H. Macromolecules 2004, 37, 8618.
16. Zheng, G. Q. A.; Huang, L.; Yang, W.; Yang, B.; Yang, M. B.; Li, Q.; Shen, C. Y. Polymer 2007, 48, 5486.
17. Liu, P.; He, G.; Wu, L. H. Mater Design 2009, 30, 2264.

18. Ratta, V.; Wilkes, G. L.; Su, T. K. Polymer 2001, 42, 9059.
19. Nagasawa, T.; Matsumura, T.; Hoshino, S.; Kobayashi, K. Appl.Polym.Symp 1973, 20, 275.
20. Keller, A.; Kolnaar, H. W. H. Mater Sci Technol Lond 1997, 18, 189.
21. Keller, A.; Machin, M. J. J Macromol Sci Phys 1967, 1, 41.
22. Giboz, J.; Copponnex, T.; Mele, P. J Micromech Microeng 2009, 19, 1.
23. Na, B.; Zhang, Q.; Fu, Q. Polymer 2002, 26, 7367.
24. Viana, J. C. Polymer 2004, 45, 993.
25. Viana, J. C.; Cunha, A. M.; Billon, N. Polymer 2002, 43, 4185.
26. Mendoza, R. Morphologies induites dans les piĕces enpolyoléfines moulées par injection. Ph.D. Thesis, ENSAM, June 2005.
27. Billon, N.; Henaff, V.; Pelous, E.; Haudin, J. M. J Appl Polym Sci 2002, 86, 725.
28. Kumaraswamy, G. J Macromol Sci Pol R C 2005, 45, 375.
29. Monasse, B. J Mater Sci 1995, 30, 5002.